Atmos. Chem. Phys. Discuss., https://doi.org/10.5194/acp-2017-902
Manuscript under review for journal Atmos. Chem. Phys.
Discussion started: 17 November 2017

Atmospheric Chemistry and Physics Discussions

Experimental study of H_2SO_4 aerosol nucleation at high ionization levels

Maja Tomicic [1], Martin Bødker Enghoff [1], and Henrik Svensmark [1]

[1]National Space Institute, Danish Technical University, Elektrovej 327, Kgs. Lyngby, Denmark

Abstract. One hundred and ten direct measurements of aerosol nucleation rate at high ionization levels were performed in an 8 m^3 reaction chamber. Neutral and ion-induced particle formation from sulphuric acid (H_2SO_4) as a function of ionization and H_2SO_4 concentration was studied. Other species that could participate in the nucleation were not measured. The measurements extend the parameter space of measurements described by Dunne et al. (2016) (at T=295 K and RH=38%) by expanding to lower H_2SO_4 concentrations ($4 \cdot 10^6$ - $3 \cdot 10^7$ cm^{-3}) and higher ion concentrations (1700 - 19000 cm^{-3}). The ion concentrations, which correspond to levels caused by a nearby supernova, were achieved with gamma ray sources. Nucleation rates were directly measured with a particle size magnifier (PSM Airmodus A10) at a size close to critical cluster size (mobility diameter of ∼1.4 nm) and formation rates at mobility diameter of ∼4 nm were measured with a CPC (TSI model 3775). The measurements show that nucleation increases by around a factor of five when the ionization increases from background to supernova levels under fixed gas conditions. The results expand the parametrization from Dunne et al. (2016) to lower sulphuric acid concentrations and higher ion concentrations.

1 Introduction

Secondary aerosol particles, that are formed by nucleation processes in the atmosphere, play an important role in atmospheric chemistry and in Earth's climate system. They affect Earth's radiation balance by scattering solar radiation back to space and can also act as cloud condensation nuclei (CCN) and thereby affect the amount and radiative properties of clouds. Clouds have a net cooling effect on Earth's radiation budget of about -27.7 W m^{-2} (Hartmann, 1993). Thus, a small change in cloud properties can have significant effect on the climate system. Results by e.g Merikanto et al. (2009) and Yu and Luo (2009) have shown that a significant fraction (ranging between 31-70%) of cloud-forming aerosol particles in the atmosphere are secondary particles that originate from nucleation. Therefore, understanding nucleation is crucial in order to fully understand the atmospheric and climatic effects of aerosols.

Sulphuric acid (H_2SO_4) is the primary ingredient in the production of secondary aerosols because of its low vapor pressure and its ability to bond with water, which is ubiquitous in the atmosphere (Curtius, 2006). H_2SO_4 is primarily produced in the atmosphere from sulphur dioxide (SO_2) via oxidation by the OH radical, produced photochemically with ultraviolet light coming from the Sun. When H_2SO_4 collides with other molecules, it starts forming small clusters of molecules that can grow into new stable aerosols. If only H_2O and H_2SO_4 take part, the process is termed binary homogeneous nucleation. Nucleation can

Atmos. Chem. Phys. Discuss., https://doi.org/10.5194/acp-2017-902
Manuscript under review for journal Atmos. Chem. Phys.
Discussion started: 17 November 2017

Atmospheric Chemistry and Physics Discussions

be significantly enhanced by other substances, the dominant ones being ammonia (NH_3) and organic molecules (Kirkby et al., 2011; Dunne et al., 2016). These processes are termed ternary and organic-mediated nucleation, respectively. Recent results show that in low H_2SO_4 environments nucleation also happens by condensation of highly oxygenated organic molecules alone (Bianchi et al., 2016). Further, ions enhance the nucleation process by stabilizing the molecular clusters, this process is termed ion-induced nucleation. The fraction of ion-induced nucleation of total particle formation was observed in various environments by Manninen et al. (2010). This study found that the fraction was in the range 1-30% being the highest in environments with generally low nucleation rates.

Typical concentration range of gas-phase H_2SO_4 in the atmosphere is $10^6 - 10^7$ cm^{-3}. The concentrations vary with location, time of the day and outlet of SO_2, which can be both anthropogenic and natural. Ions are ubiquitous in the lower atmosphere and are mainly produced by galactic cosmic rays (GCR), forming 1-40 ion pairs $\mathrm{cm}^{-3}\mathrm{s}^{-1}$. The formation rate depends on factors such as altitude, latitude, and the solar cycle. Ionization is higher above land than above ocean due to natural radioactivity from soils, and the maximum ionization is at altitudes of ~ 13 km (Bazilevskaya et al., 2008). In addition to the natural variations in ionization, an event such as a nearby supernova would significantly increase the atmospheric ionization in the time following the event. There exists strong indications of a supernova at a relatively close distance of ~50 pc from the solar system $\sim$ 2.2 million years ago (Knie et al., 2004; Kachelrieß et al., 2015; Savchenko et al., 2015; Fimiani et al., 2016). According to Melott et al. (2017) the increase in GCR from such an event would cause an increase in tropospheric ionization of up to a factor of 50 during the first few hundred years following the event.

Few measurements exist that quantify parameters affecting and assisting nucleation (Berndt et al., 2006; Benson et al., 2011; Sipila et al., 2010; Kirkby et al., 2011; Svensmark et al., 2007; Enghoff et al., 2011; Yu et al., 2017). Recent laboratory measurements by Dunne et al. (2016) determined the dependence on temperature, trace gas and ion concentrations and provided a parametrization that can be incorporated into climate models. These and other measurements, (e.g., Svensmark et al., 2007; Enghoff et al., 2011; Kirkby et al., 2011) have verified that ionization helps the nucleation process. In this work we expand on these results by measuring nucleation at ion production rates (q) ranging from background levels to 560 $\mathrm{cm}^{-3}\mathrm{s}^{-1}$, corresponding to those following a nearby supernova, and atmospherically relevant H_2SO_4 concentrations ($4 \cdot 10^6$ - $3 \cdot 10^7$ cm^{-3}).

2 Experimental methods

The measurements presented in this work were performed in an 8 m^3 reaction chamber (SKY2). The setup is shown schematically in Fig. 1. The chamber is made of electro-polished stainless steel and has one side fitted with a Teflon foil to allow UV light (253.7 nm) to illuminate the chamber and start the photo-chemical reaction to generate H_2SO_4. The chamber was continuously flushed at a rate of 25 L min^{-1}. Dry purified air and water vapor was added to reach a relative humidity of 38%. Ozone (O_3), and sulphur dioxide (SO_2) was added to the chamber and the concentration of O_3 was measured with a

Atmos. Chem. Phys. Discuss., https://doi.org/10.5194/acp-2017-902
Manuscript under review for journal Atmos. Chem. Phys.
Discussion started: 17 November 2017

Atmospheric Chemistry and Physics Discussions

Teledyne T400 analyzer and SO_2 with a Thermo 43 CTL analyzer. The H_2SO_4 concentration was measured with a chemical ionization atmospheric pressure interface time-of-flight (CI-API-ToF) mass spectrometer (Jokinen et al., 2012). The chamber is also equipped with instruments to measure temperature, differential and absolute pressure, humidity, and UV intensity. The pressure was held at a slight (~ 0.1 mbar) overpressure, the temperature at 295 K and the UV intensity was varied as part of the experiments.

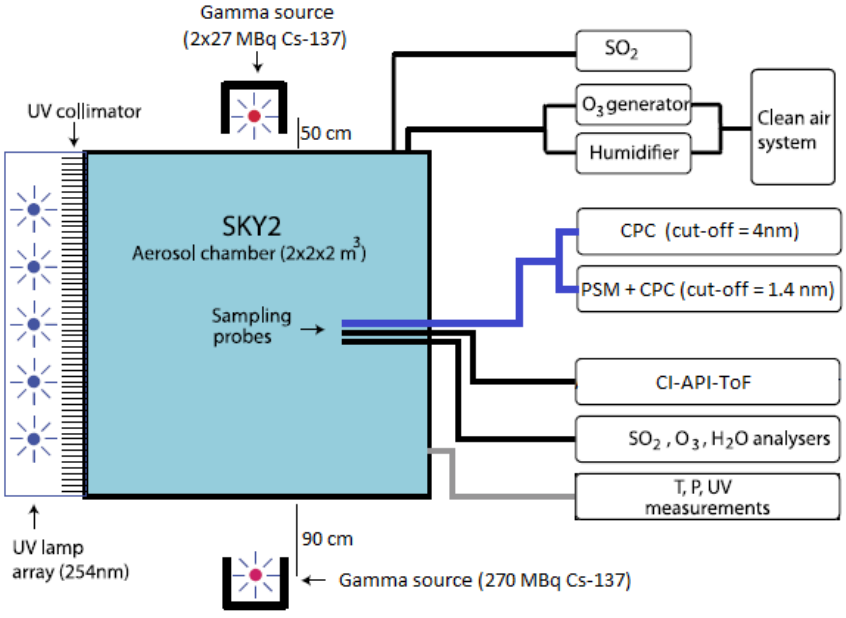

Figure 1. A schematic of the SKY2 reaction chamber and the instruments used for the experiment. The figure is an edited version of the schematic from Svensmark et al. (2013).

Two different condensation particle counters (CPCs) and a particle size magnifier (PSM) were used to count the aerosols formed in the experiments. A TSI model 3775 CPC was used to determine the aerosol particle concentration above a cutoff diameter of 4 nm ($d_{\mathrm{p,cutoff}}$ = 4 nm). And a TSI 3776 CPC ($d_{\mathrm{p,cutoff}}$ = 2.5 nm) was used in series with the PSM Airmodus A10, developed and described by (Vanhanen et al., 2011), to detect particles above a cut-off diameter of $\sim$1.4 nm. The cut-off diameter is defined as the mobility diameter of particles of which 50% are counted and it depends on the saturator flow rate and the chemical composition of the particles. For the PSM, the saturator flow rate was set to 1.3 L min^{-1} which corresponds to a cut-off diameter of 1.4 nm for tungstenoxide particles. The cut-off for H_2SO_4 aerosols is not known exactly. The cut-off diameter of the PSM is very close to the critical size of $\sim$1.5 nm (Kirkby et al., 2011) which allows for direct measurements of nucleation rate thereby avoiding extrapolations of the nucleation rate from larger sizes (Kürten et al., 2017). Both instruments (PSM and CPC) sampled from the same line and had identical sampling pathways as illustrated in Fig. 1. The CPC with the larger cut-off diameter was used on its own to achieve a larger size span between the instruments which enables the determination of the particle growth rate (GR).

Atmos. Chem. Phys. Discuss., https://doi.org/10.5194/acp-2017-902
Manuscript under review for journal Atmos. Chem. Phys.
Discussion started: 17 November 2017

Atmospheric Chemistry and Physics Discussions

2.1 Ionization of Air by Gamma Sources

The air in the 8 m^3 reaction chamber was ionized by gamma sources. Enghoff et al. (2011) have shown that the nature of the ionizing particles is not important for the nucleation of aerosols. Therefore, even though particles from an accelerator beam can have energies closer to GCR, gamma radiation, which is more accessible, can be used to study the ion-induced nucleation. Three Cs-137 sources were used in the setup; two 27 MBq and one 270 MBq. To achieve a homogeneous radiation of the chamber, the 270 MBq source was placed on one side of the chamber, at a ~ 90 cm distance, and the two 27 MBq sources were placed close to each other on the opposite side of the chamber, at ~ 50 cm distance. The setup is illustrated in Fig. 1. Ions are also produced in the chamber by naturally occurring GCR and background radiation from Radon at a rate of ~ 3 $cm^{-3}s^{-1}$. In order to perform measurements at different ionization levels, lead shielding of varying thickness was placed in front of the sources. Four ionization levels were achieved by using either 0 cm, 1.5 cm, 3.5 cm, or 8.5 cm lead shielding.

The uniformity and level of the ionization caused by the sources was estimated from simulations in Geant 4, with the G4beamline program (CMS Groupware, 2017). Figure 2 shows the ionization rates (q) in the chamber caused by the gamma sources, for minimum and maximum shielding thickness. The graphs show the chamber as seen from opposite the UV lamps. Thus, the 270 MBq source is on the left side of the graphs. From the simulation results in Fig. 2, it is clear that when the gamma sources were fully exposed the 270 MBq source created more ion pairs than the two weaker sources on the opposite side of the chamber. The variation from highest to lowest ionization is around a factor of two which translates into a factor 1.4 in ion concentration. There is some circulation of the air in the chamber and the air is sampled from approximately in the middle between the sources as seen in Fig. 1, therefore it is assumed that the average ionization is a good representation of the ionization of the sampled air.

Atmos. Chem. Phys. Discuss., https://doi.org/10.5194/acp-2017-902
Manuscript under review for journal Atmos. Chem. Phys.
Discussion started: 17 November 2017

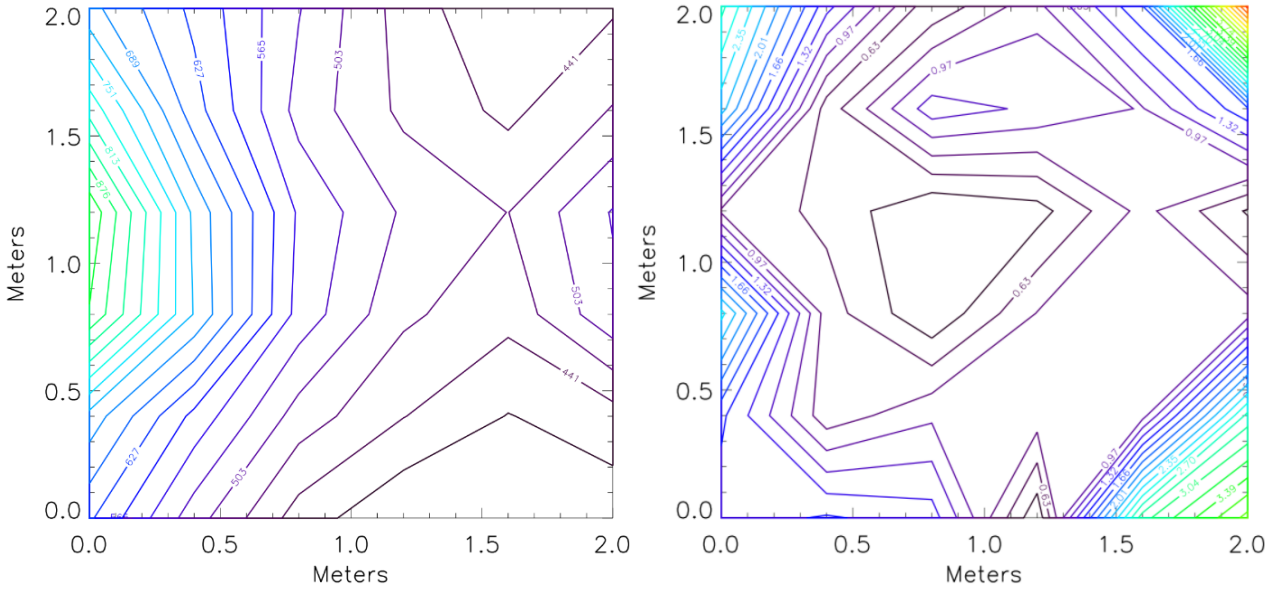

Figure 2. Geant 4 simulations of ionization rate, q [cm^{-3}s^{-1}], in the chamber with 0 cm (left) and 8.5 cm (right) lead shielding. The average ionization is presented in Table 1.

Table 1. Average ionization rate (q) achieved with the gamma sources at various thickness of lead shielding calculated with Geant 4. Ion density (N) including the ions produced by naturally occurring radiation.

Shielding thickness	8.5 cm	3.5 cm	1.5 cm	0 cm
q [cm^{-3}s^{-1}]	1.4	10	109	560
N [cm^{-3}]*	1700	2900	8400	$1.9 \cdot 10^4$

* Approximate values calculated with $N = \sqrt{q_{\mathrm{total}}/\alpha}$, where α=1.6·10^{-6} is the recombination coefficient and q_{total} is the sum of the natural ionization (3 cm^{-3}s^{-1}) and the enhanced ionization caused by the sources.

2.2 Design of Experiments

The experiments were conducted by turning on the UV lamps for 20 minutes to generate H_2SO_4. The [H_2SO_4] depends on the intensity of the UV light, thus, by varying the intensity between experiments, the H_2SO_4 concentration was varied. Once sufficient H_2SO_4 was present, nucleation started and continued until the H_2SO_4 was used up and/or lost to the chamber walls. The aerosol formation rate was measured at the respective cut-off diameters with the PSM and CPC. The procedure lasted six to fourteen hours for a single run under fixed gas conditions, depending on the sulphuric acid concentration, because the system had to return to its initial conditions (PSM concentration < 2 cm^{-3}) before a new experiment was started. In between experiments, the ionization conditions were varied by changing the amount of lead shielding in front of the gamma sources. At

Atmos. Chem. Phys. Discuss., https://doi.org/10.5194/acp-2017-902
Manuscript under review for journal Atmos. Chem. Phys.
Discussion started: 17 November 2017

Atmospheric Chemistry and Physics Discussions

least one hour before each experiment the lead shielding was put in the right position to allow the ionization level to stabilize before the nucleation started.

The upper limit to the H_2SO_4 concentrations was chosen based on time constraints, because too high concentrations yielded a particle count which took a long time to decay back to initial conditions (< 2 cm^{-3}). The lower limit of the H_2SO_4 concentrations was chosen based on the detection limit of the instrument. The CPC with cut-off diameter of 4 nm was the limiting instrument because the majority of the particles are lost during the growth from 1.4 to 4 nm. On average, 25% of the particles survive the growth. The survival is only 10% for low H_2SO_4 concentrations since the growth rate (GR) is slower in this case.

Every fifth measurement was performed as a reference experiment with a standard ion concentration (N = 2900 $cm^{-3}s^{-1}$) and UV intensity (20 %), to avoid unnoticed drift in parameters or instruments. The reference experiments showed that the [H_2SO_4] varied despite of the identical UV setting because the O_3 concentration decreased during the measurement series. This drift was caused by the O_3 generator, in which a UV lamp was replaced immediately prior to the measurements series. The lamp intensity decreased with time causing smaller H_2SO_4 concentrations for a given UV setting. A list of settings and the number of measurements at each setting is presented in Table 2.

Table 2. The range of UV and radiation level settings that were varied through the measurement series. The radiation levels are: 0 : N = 1700 cm^{-3}, 1 : N = 2900 cm^{-3}, 2 : N = 8400 cm^{-3}, 3 : N = 19000 cm^{-3}. The last column shows the number of measurements at each setting. The reference measurements were performed at 20 % UV and radiation level 1.

UV intensity	Radiation level	# of Measurements
15 %	0/1/2/3	5/4/2/5
18 %	0/1/2/3	2/0/0/2
20 %	0/1/2/3	5/18/3/8
22 %	0/1/2/3	4/3/3/5
25 %	0/1/2/3	2/3/3/5
30 %	0/1/2/3	3/2/0/3
35 %	0/1/2/3	1/3/0/3
40 %	0/1/2/3	2/2/0/2
45 %	0/1/2/3	2/2/0/3

Atmos. Chem. Phys. Discuss., https://doi.org/10.5194/acp-2017-902
Manuscript under review for journal Atmos. Chem. Phys.
Discussion started: 17 November 2017

Atmospheric Chemistry and Physics Discussions

3 Data processing

3.1 Sulphuric Acid Measurements

The CI-API-ToF mass spectrometer was used to determine the concentration of H_2SO_4. The CI-API-ToF spectrometer used in the setup was calibrated with the calibration system presented in Kürten et al. (2012). We use the calibration coefficient, C, as defined in Eq. (1) in Jokinen et al. (2012):

$$[H_2SO_4] = \frac{HSO_4^- + HSO_4^- \cdot HNO_3}{NO_3^- + NO_3^- HNO_3 + NO_3^- (HNO_3)_2} \cdot C \quad (1)$$

The resulting calibration coefficient was C=$9.86 \cdot 10^9 \pm 4.22 \cdot 10^8$ molec cm^{-3}. Values in the literature vary from $5 \cdot 10^9$ to $1.89 \cdot 10^{10}$ molec cm^{-3} (Kürten et al., 2012). The concentrations measured directly by the mass spectrometer are integrated concentrations of masses over a small region (± 0.5 AMU) of the spectrum. This means that the concentrations are overestimated because they include noise around the actual peak. This was also taken into account and corrected for using the results from Hansen (2016).

The mean peak concentration is determined by using a 50 point moving average. In addition to the uncertainty in the calibration factor there is a statistical uncertainty related to the determination of the mean peak concentration. This uncertainty arises from the fluctuations in the non-smoothed data and was therefore calculated from the standard error of the mean of the 50 points.

The CI-API-ToF mass spectrometer broke down during the measurement series. Therefore, 60 out of 110 experiments do not include direct measurements of the H_2SO_4 concentration. For these experiments, the concentration was interpolated from a linear relation between the H_2SO_4 concentration, in the 50 direct measurements, and the GR of the aerosol particles, see Sect. 3.2. Previously, linear relations between GR and H_2SO_4 have been demonstrated by e.g., Kulmala et al. (2003).

3.2 Determination of Growth rate

The different cut-off diameters of the PSM A10 (1.4 nm) and TSI model 3775 CPC (4 nm) allow for a GR to be calculated from the time difference, Δt, between measurements in the two instruments. We use a percentage limit (50% of the maximum concentration) instead of absolute numbers to take particle losses during growth into account. The difference in the cut-off diameters of the two instruments is 2.6 nm. The GR is therefore defined as:

$$GR = \frac{2.6\text{nm}}{\Delta t} \quad (2)$$

The calculated GR were in the interval 14-34 nm h^{-1} at H_2SO_4 concentration ranging from $7.2 \cdot 10^6$ to $2.7 \cdot 10^7$ cm^{-3}. These GR values are reasonable compared to atmospheric GR ($\sim$ 1-20 nm^{-1}) (Kulmala et al., 2004). We note that although the GR

Atmos. Chem. Phys. Discuss., https://doi.org/10.5194/acp-2017-902
Manuscript under review for journal Atmos. Chem. Phys.
Discussion started: 17 November 2017

Atmospheric Chemistry and Physics Discussions

are higher than expected from pure sulphuric acid condensation at the kinetic limit indicating the participation of other vapours in the early growth (Tröstl et al., 2016) we still find a linear relationship between sulphuric acid and the GR.

3.3 Determination of Nucleation Rate

Nucleation rates, J_D, were measured at a mobility diameter of $D \sim$1.4 nm with the PSM A10. The particle diameter of 1.4 nm comes close to the critical cluster size and therefore the PSM allows for direct measurements of the nucleation rate. The PSM measures the concentration of particles with diameters above the cut-off, $N_{1.4}$. The nucleation rate is defined as: $J_{1.4} = dN_{1.4}/dt$ and was determined by calculating the gradient of the area between the 20% and 80% of each peak of particle concentration. Therefore, we use the standard deviation on the gradient as the one σ error on the nucleation rate.

The nucleation rates as a function of H_2SO_4 and ion concentrations are seen in Fig. 3 with one σ errorbars. The errorbars on the H_2SO_4 and $J_{1.4}$ are the statistical standard errors. The Poisson counting uncertainty for the PSM ($\sqrt{N}$ (see Sect. 3.4)) and the calibration uncertainty for the mass spectrometer ($\sim 5\%$) are not shown.

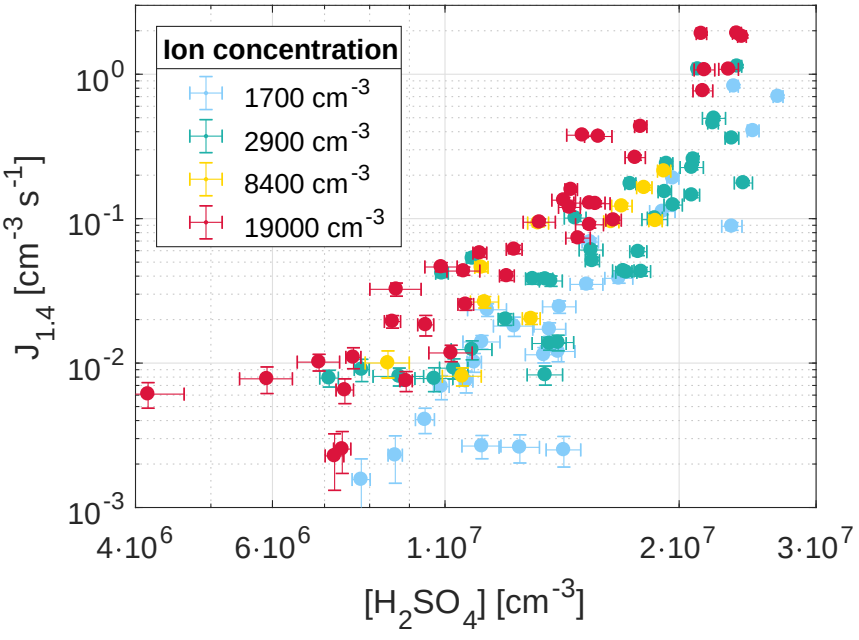

Figure 3. Nucleation rates as a function of sulphuric acid concentration and ion concentration. The errorbars represent one σ standard deviation.

Atmos. Chem. Phys. Discuss., https://doi.org/10.5194/acp-2017-902
Manuscript under review for journal Atmos. Chem. Phys.
Discussion started: 17 November 2017

Atmospheric Chemistry and Physics Discussions

3.4 Additional Uncertainties

Additional uncertainties in the particle concentration measurement arise, for example, from low particle counting statistics, from chemical composition dependent variation in the cutoff diameter of the particle counters, and from loss of particles in the sampling system. According to Kangasluoma and Kontkanen (2017) particle sampling and counting is a Poisson process and the statistical uncertainty is determined from the Poisson counting uncertainty, $\sqrt{N}$, which describes the standard deviation, σ, of the counted particles, N. Losses due to dilution, coagulation and deposition on chamber walls are not considered since the particle concentration is measured close to the critical size.

Aerosols are lost to the walls of the sampling system due to diffusion. This type of loss is size dependent and was estimated using the Particle Loss Calculater (PLC) developed by von der Weiden et al. (2009). The loss function estimates that the losses of the 1.4 nm particles in the sampling system are $\sim$50% and only $\sim$15% for the 4 nm particles. Since we do not measure the particle size distribution diffusion losses are not included directly in the data analysis. This means that we could have underestimated the concentration of the smallest aerosols and thereby the nucleation rates.

4 Results and Discussion

To quantify the nucleation we adopt the parametrization presented in Dunne et al. (2016) and thus represent the nucleation as a sum of binary (b), ternary (t), neutral (n), ion-induced (i), and organic nucleation (org). The term representing the organic nucleation rate is not used, as this study does not intentionally add or measure organic molecules. Atmospheric concentrations of methane are expected within the chamber but these are not expected to affect nucleation. There might be traces of other organic species that contribute to the nucleation rate. The concentrations are considered constant and are included in the ternary nucleation rate to reduce the number of fitting parameters. Thus, a nucleation rate given by the sum of the four contributions is considered:

$$J = J_{b,n} + J_{t,n} + J_{b,i} + J_{t,i} \tag{3}$$

Ammonia (NH_3) is filtered from the air that enters the chamber with a citric acid filter. However, trace amounts are still present in the chamber and contribute to the production of stable clusters. As the concentration is not measured, the two ternary processes involving NH_3 are not directly fitted from the data. Instead, they are included in the modelling by assuming that the concentration of NH_3 and organic molecules is constant in all measurements. Thereby, it can be determined from a comparison of the results obtained in this study with the results from Dunne et al. (2016) under the same conditions (including T=295 K, RH=38%, and N=1700 cm^{-3} in both studies). Figure 4 shows the parametrization from Dunne et al. (2016) on top of the data from our experiments with the NH_3 concentration set at $3{\cdot}10^{10}$ cm^{-3} (1.2 ppbv), for N=1700 cm^{-3} (left) and all ionization levels (right). Since [NH_3]=$3{\cdot}10^{10}$ cm^{-3} is the value that gives the best match between data (see Fig. 4) and the extrapolated parametrization (dashed lines) it is assumed to represent the concentration of NH_3 and organic species. Atmospherically observed NH_3 concentrations are typically at the sub-ppbv and ppbv level (Erupe et al., 2010; Nowak et al., 2006). We note that

Atmos. Chem. Phys. Discuss., https://doi.org/10.5194/acp-2017-902
Manuscript under review for journal Atmos. Chem. Phys.
Discussion started: 17 November 2017

Atmospheric Chemistry and Physics Discussions

nucleation rates were reported for a mobility diameter of 1.7 nm in Dunne et al. (2016) meaning that the rates measured in this study should be slightly overestimated since we measure at a mobility diameter of 1.4 nm.

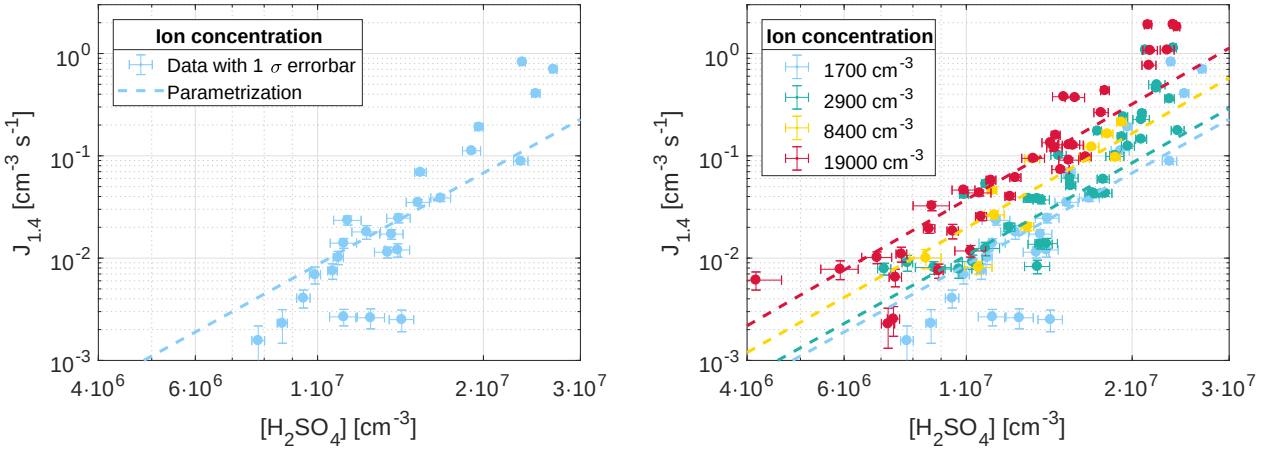

Figure 4. Parametrization from Dunne et al. (2016) with [NH_3]=1.2 ppb (dashed lines) and nucleation rate measurements from this study at T=295 K, RH=38%, N=1700 cm^{-3} (left) and all N (right).

As seen from Fig. 4 the parametrization presented in Dunne et al. (2016) matches the nucleation rates from this study, when extrapolated to the same region, especially at [H_2SO_4] < $2 \cdot 10^7$ cm^{-3}. At higher values of [H_2SO_4] the nucleation rates from this study are higher than expected from the parametrization. The disagreement is further quantified by fitting the nonlinear function in Eq. (3) to the experimental data from this study. The two terms that represent the binary nucleation are given by:

$$J_{b,n} = k_{b,n}(T)[H_2SO_4]^{p_{b,n}} \tag{4}$$

and

$$J_{b,i} = k_{b,i}(T)n_-[H_2SO_4]^{p_{b,i}} \tag{5}$$

Where $J_{b,n}$ is the binary neutral rate and $J_{b,i}$ is the binary ion-induced rate, with n_- being the negative ion concentration. In this study the temperature is not varied, therefore the coefficients $k(T)$ that account for the temperature dependence, are constant and can also be calculated by extrapolation from Dunne et al. (2016, Sup. Mat.) to our region of [H_2SO_4], N, T, and RH. Thus, we fit Eq. (3) to estimate the parameters $p_{b,n}$ and $p_{b,i}$ for high ionization levels.

Atmos. Chem. Phys. Discuss., https://doi.org/10.5194/acp-2017-902
Manuscript under review for journal Atmos. Chem. Phys.
Discussion started: 17 November 2017

Atmospheric Chemistry and Physics Discussions

The nonlinear fit was performed using a Levenberg-Marquardt algorithm in Matlab in order to find the best R^2 coefficient. The fit was weighted in order to include the standard deviation on the data. The best fit parameters are $p_{b,n} = 10.68$ and $p_{b,i} = 6.33$ for $J_{b,n}$ and $J_{b,i}$ respectively (R^2=0.77). Figure 5 shows the best fit parametrization and Table 3 lists all parameters.

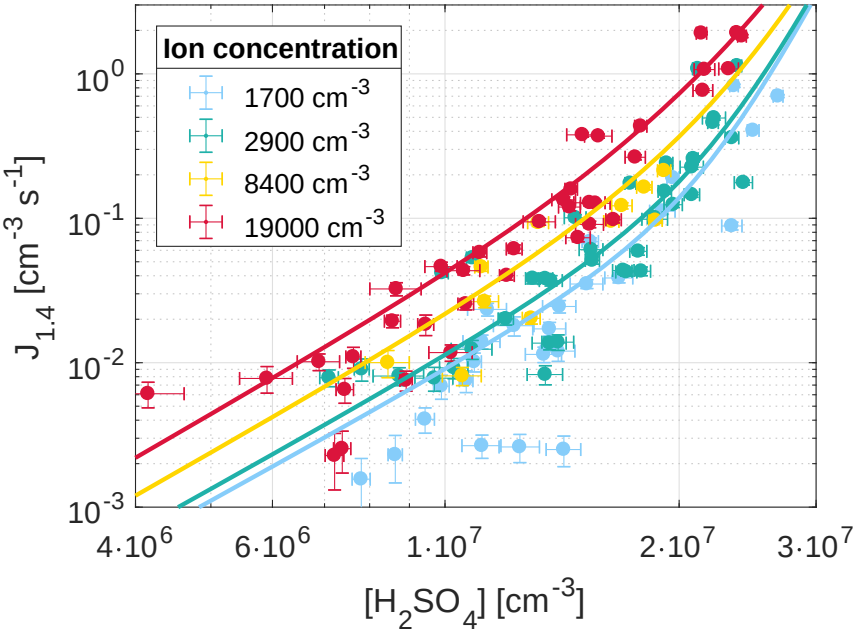

Figure 5. Best fit of the parametrization to the experimental data. The parameters are presented in Table 3.

Table 3. The second column presents the best fit parameters for neutral and ion-induced nucleation. The fit is performed with sulphuric acid and ammonia concentrations in units of 10^6 cm^{-3}. The third column shows the parameters from Dunne et al. (2016) for comparison.

Parameters	This study	Dunne et al. (2016)
$k_{b,n}$ *	4.79e-16	4.79e-16
$p_{b,n}$	10.68	3.95
$k_{b,i}$ *	1.14e-13	1.14e-13
$p_{b,i}$	6.33	3.37

* Values are extrapolated from Dunne et al. (2016).

The resulting parametrization shows that at an atmospherically relevant H_2SO_4 concentration of $1 \cdot 10^7 \mathrm{cm}^{-3}$ the increase in ions from background levels to the highest measured levels causes an increase in nucleation rate of around a factor five.

Atmos. Chem. Phys. Discuss., https://doi.org/10.5194/acp-2017-902
Manuscript under review for journal Atmos. Chem. Phys.
Discussion started: 17 November 2017

Atmospheric Chemistry and Physics Discussions

The slopes for Log $J_{1.4}$ vs. Log [H_2SO_4] for fixed ion conditions, when only the binary term given by Eq. (4) is considered, were also calculated. The results are 5.1 ±0.3 for ionization level 0, 3.3 ±0.3 for level 1, 3.1 ±0.8 for level 2, and 4.7 ±0.3 for the highest ionization.

The disagreement between the data and the expected parametrization could be caused by the narrow range of [H_2SO_4] in this study, which are all within one order of magnitude. Another explanation could be because the detection efficiency of the PSM is ∼50% for particles close to the critical size of 1.4 nm. Since we use a percentage region instead of a fixed time interval when calculating the nucleation rate (see Sect. 3.3), it is possible that the parameters p and the slopes of Log J vs. Log [H_2SO_4] were overestimated due to the lower detection efficiency of PSM for particles smaller than 2 nm. At higher [H_2SO_4], more particles could grow into sizes that are detected more efficiently by the PSM compared to at lower [H_2SO_4]. This was taken into account by verifying that the regions between 20% and 80% of each peak of particle concentration were linear. If the detection efficiency was dependent on [H_2SO_4] these regions would not be linear but the gradient would increase with time for a given peak. However, we still note that the detection efficiency of the PMS could have affected the results in another way. Likewise, it is worth noting that the effect of ions on the detection efficiency of the PSM is unknown, but ions may be more efficiently detected (Winkler et al., 2008).

From the best fit of the parametrization, the exponent on the neutral nucleation rate, $p_{b,n}$, is higher than the ion induced, $p_{b,i}$. This suggest, as expected, that ions stabilize the clusters, suggesting that fewer H_2SO_4 molecules are needed to form a stable cluster when ions are present. When the experiments where fitted separately for each individual ion condition, the slope on the H_2SO_4 dependence did not show systematic variation with ion concentration. The highest slope was at lowest ion levels as expected, however, the two middle ion levels showed significantly lower slopes than at level 0 and level 3. We believe that the explanation is in the small range of sulphuric acid concentrations.

Figure 6 shows the individual contributions (from Eq. (3)) to the total nucleation rate for ionization level 1. From this we see that high values of the two p-exponents resulting from the fit (second column in Table 3), compared to results from Dunne et al. (2016) (third column in Table 3), can be explained mathematically by the fact that the ternary terms describes most of the nucleation and we therefore only fit the steep increase in nucleation rate for [H_2SO_4] > $2 \cdot 10^7$ cm^{-3}.

In order to fully account for the variables in nucleation processes observed in this study, direct measurement of NH_3 and organic substances would have been preferred. Nonetheless, a consistency with the results from Dunne et al. (2016) is shown.

5 Conclusions

The nucleation of H_2SO_4/H_2O aerosols was studied under near-atmospheric conditions in an 8 m^3 reaction chamber. Sulphuric acid was produced in situ in the range [H_2SO_4]= $4 \cdot 10^6$ - $3 \cdot 10^7$ cm^{-3} and the ionization of the air in the chamber was increased from background levels of ∼ 4 cm^{-3}s^{-1} up to 560 cm^{-3}s^{-1} (ion concentrations = 1700 - 19000 cm^{-3}) using gamma sources.

Atmos. Chem. Phys. Discuss., https://doi.org/10.5194/acp-2017-902
Manuscript under review for journal Atmos. Chem. Phys.
Discussion started: 17 November 2017

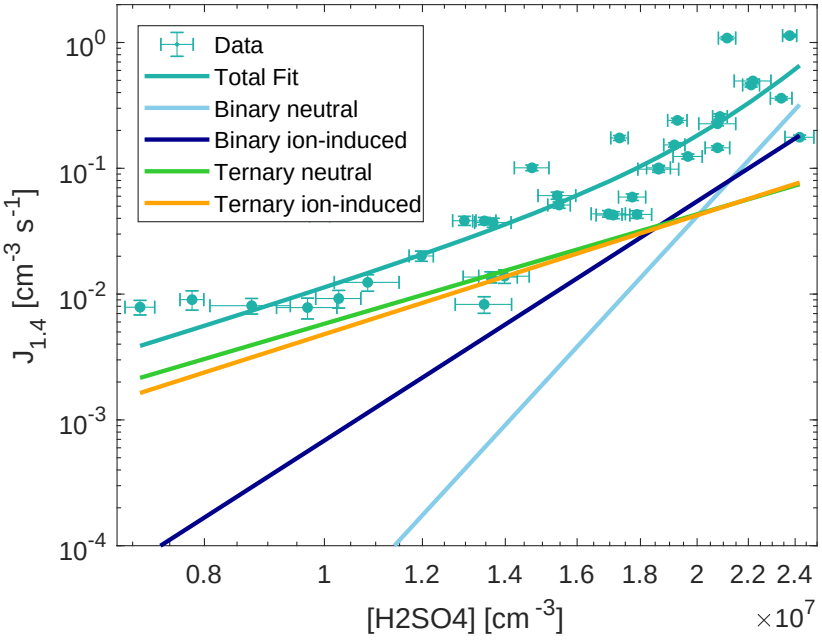

Figure 6. Individual contributions ($J_{b,n}$, $J_{b,i}$, $J_{t,n}$ and $J_{t,i}$) to the total nucleation rate ($J_{1.4}$), for ionization level 1.

Such levels of ionization are relevant for e.g. a nearby ($\sim$ 50 pc) supernova which is thought to have occurred $\sim$2.2 million years ago. The experiments were performed at T=295 K and RH=38%. The study shows that nucleation increases linearly with ion concentration, over the full range of ion concentrations. And, we find that nucleation increases by a factor of five, when the ion concentration is increased from background to maximum levels. Further, the dependence of the nucleation rate on [H_2SO_4] is in the range 3-5 when only the binary nucleation rate is considered. This dependency could be overestimated because of the narrow range of [H_2SO_4] which is within one order of magnitude. We have not measured the concentration of other nucleating species than sulphuric acid. Still, this study is a novel contribution to the experimental studies of nucleation rates for the ammonia/organic-mediated H_2SO_4/H_2O system because of the direct measurements of nucleation rates at sizes close to the critical cluster size at high ion concentrations. Based on the presented experiments we find it reasonable to expand the parametrization from Dunne et al. (2016) to lower sulphuric acid concentrations and higher ion concentrations.

Data availability. The datasets generated and analysed during the current study are available from the corresponding author on request.

Author contributions. M. Tomicic co-designed and co-performed the experiments, performed the data analysis and wrote the paper. M. B. Enghoff co-designed and co-performed the experiments and provided input to the data analysis and paper. H. Svensmark provided input to all parts of the work.

Competing interests. The authors declare no competing interests.

Acknowledgements. We thank Mikael Jensen and DTU NUTECH for lending us the 270 MBq Cs-137 source and for help with the transport. We thank Andreas Kürten for lending us his model for the calibration of the CI-API-ToF. We thank Knud Højgaards Foundation for funding the TSI 3776 CPC.

References

Bazilevskaya, G. A., Usoskin, I. G., Flückiger, E. O., et al.: Cosmic Ray Induced Ion Production in the Atmosphere, Space Science Reviews, 137, 149–173, https://doi.org/10.1007/s11214-008-9339-y, https://doi.org/10.1007/s11214-008-9339-y, 2008.

Benson, D. R., Yu, J. H., Markovich, A., and Lee, S.-H.: Ternary homogeneous nucleation of H_2SO_4, NH_3, and H_2O under conditions relevant to the lower troposphere, Atmospheric Chemistry and Physics, 11, 4755–4766, https://doi.org/10.5194/acp-11-4755-2011, https://www.atmos-chem-phys.net/11/4755/2011/, 2011.

Berndt, T., Böge, O., and Stratmann, F.: Formation of atmospheric H2SO4/H2O particles in the absence of organics: A laboratory study, Geophysical Research Letters, 33, n/a–n/a, https://doi.org/10.1029/2006GL026660, http://dx.doi.org/10.1029/2006GL026660, l15817, 2006.

Bianchi, F., Tröstl, J., Junninen, H., et al.: New particle formation in the free troposphere: A question of chemistry and timing, Science, 352, 1109–1112, https://doi.org/10.1126/science.aad5456, http://science.sciencemag.org/content/352/6289/1109, 2016.

CMS Groupware: G4-Beamline open source software, http://www.muonsinternal.com/muons3/G4beamline, 2017.

Curtius, J.: Nucleation of atmospheric aerosol particles, Comptes Rendus Physique, 7, 1027 – 1045, https://doi.org/https://doi.org/10.1016/j.crhy.2006.10.018, http://www.sciencedirect.com/science/article/pii/S1631070506002301, nucleation, 2006.

Dunne, E. M., Gordon, H., Kürten, A., et al.: Global atmospheric particle formation from CERN CLOUD measurements, Science, 354, 1119–1124, https://doi.org/10.1126/science.aaf2649, http://science.sciencemag.org/content/354/6316/1119, 2016.

Enghoff, M. B., Pedersen, J. O. P., Uggerhøj, et al.: Aerosol nucleation induced by a high energy particle beam, Geophysical Research Letters, 38, n/a–n/a, https://doi.org/10.1029/2011GL047036, http://dx.doi.org/10.1029/2011GL047036, l09805, 2011.

Erupe, M. E., Benson, D. R., Li, J., et al.: Correlation of aerosol nucleation rate with sulfuric acid and ammonia in Kent, Ohio: An atmospheric observation, Journal of Geophysical Research: Atmospheres, 115, n/a–n/a, https://doi.org/10.1029/2010JD013942, http://dx.doi.org/10.1029/2010JD013942, d23216, 2010.

Fimiani, L., Cook, D. L., Faestermann, T., Gómez-Guzmán, J. M., Hain, K., Herzog, G., Knie, K., Korschinek, G., Ludwig, P., Park, J., Reedy, R. C., and Rugel, G.: Interstellar ^{60}Fe on the Surface of the Moon, Phys. Rev. Lett., 116, 151 104, https://doi.org/10.1103/PhysRevLett.116.151104, https://link.aps.org/doi/10.1103/PhysRevLett.116.151104, 2016.

Hansen, N.: Analysis of CI API-ToF mass spectrometer data from an atmospheric reaction chamber, Bachelor's thesis, National Space Institute, Danish Technical Univertsity, Denmark, 2016.

Hartmann, D. L.: Radiative effects of clouds on earth's climate, in: Aerosol–Cloud–Climate Interactions, edited by Hobbs, P. V., vol. 54, pp. 151–173, Academic Press, 1993.

Jokinen, T., Sipilä, M., Junninen, H., et al.: Atmospheric sulphuric acid and neutral cluster measurements using CI-APi-TOF, Atmospheric Chemistry and Physics, 12, 4117–4125, https://doi.org/10.5194/acp-12-4117-2012, http://www.atmos-chem-phys.net/12/4117/2012/, 2012.

Kachelrieß, M., Neronov, A., and Semikoz, D. V.: Signatures of a Two Million Year Old Supernova in the Spectra of Cosmic Ray Protons, Antiprotons, and Positrons, Phys. Rev. Lett., 115, 181 103, https://doi.org/10.1103/PhysRevLett.115.181103, https://link.aps.org/doi/10.1103/PhysRevLett.115.181103, 2015.

Kangasluoma, J. and Kontkanen, J.: On the sources of uncertainty in the sub-3nm particle concentration measurement, Journal of Aerosol Science, 112, 34 – 51, https://doi.org/https://doi.org/10.1016/j.jaerosci.2017.07.002, http://www.sciencedirect.com/science/article/pii/S002185021730054X, 2017.

Kirkby, J., Curtius, J., Almeida, J., Dunne, E., et al.: Role of sulphuric acid, ammonia and galactic cosmic rays in atmospheric aerosol nucleation, Nature, 476, 429–433, https://doi.org/10.1038/nature10343, 2011.

Knie, K., Korschinek, G., Faestermann, T., Dorfi, E. A., et al.: ^{60}Fe Anomaly in a Deep-Sea Manganese Crust and Implications for a Nearby Supernova Source, Phys. Rev. Lett., 93, 171 103, https://doi.org/10.1103/PhysRevLett.93.171103, http://link.aps.org/doi/10.1103/PhysRevLett.93.171103, 2004.

Kulmala, M., Dal Maso, M., Mäkelä, J., Pirjola, L., et al.: On the formation, growth and composition of nucleation mode particles, 53, 479 – 490, 2003.

Kulmala, M., Vehkamäki, H., Petäjä, T., Maso, M. D., et al.: Formation and growth rates of ultrafine atmospheric particles: a review of observations, Journal of Aerosol Science, 35, 143 – 176, https://doi.org/https://doi.org/10.1016/j.jaerosci.2003.10.003, http://www.sciencedirect.com/science/article/pii/S0021850203004373, 2004.

Kürten, A., Rondo, L., Ehrhart, S., and Curtius, J.: Calibration of a Chemical Ionization Mass Spectrometer for the Measurement of Gaseous Sulfuric Acid, J. Phys. Chem. A, 116, 6375–6386, https://doi.org/doi:10.1021/jp212123n, 2012.

Kürten, A., Li, C., Bianchi, F., Curtius, J., et al.: New particle formation in the sulfuric acid-dimethy lamine-water system: Reevaluation of CLOUD chamber measurements and comparison to an aerosol nucleation and growth model, pp. 1–31, 2017.

Manninen, H. E., Nieminen, T., Asmi, E., Gagné, S., et al.: EUCAARI ion spectrometer measurements at 12 European sites – analysis of new particle formation events, Atmospheric Chemistry and Physics, 10, 7907–7927, https://doi.org/10.5194/acp-10-7907-2010, https://www.atmos-chem-phys.net/10/7907/2010/, 2010.

Melott, A. L., Thomas, B. C., Kachelrieß, M., Semikoz, D. V., and Overholt, A. C.: A Supernova at 50 pc: Effects on the Earth's Atmosphere and Biota, The Astrophysical Journal, 840, 105, http://stacks.iop.org/0004-637X/840/i=2/a=105, 2017.

Merikanto, J., Spracklen, D. V., Mann, G. W., Pickering, S. J., and Carslaw, K. S.: Impact of nucleation on global CCN, Atmospheric Chemistry and Physics, 9, 8601–8616, https://doi.org/10.5194/acp-9-8601-2009, https://www.atmos-chem-phys.net/9/8601/2009/, 2009.

Nowak, J. B., Huey, L. G., Russell, A. G., Tian, D., et al.: Analysis of urban gas phase ammonia measurements from the 2002 Atlanta Aerosol Nucleation and Real-Time Characterization Experiment (ANARChE), J. Geophys. Res., 111, https://doi.org/doi:17310.11029/12006JD007113, 2006.

Savchenko, V. et al.: Imprint of a 2 Million Year Old Source on the Cosmic-Ray Anisotropy, The Astrophysical Journal, 809, https://doi.org/https://doi.org/10.1088/2041-8205/809/2/L23, 2015.

Sipila, M., Berndt, T., Petaja, T., et al.: The Role of Sulfuric Acid in Atmospheric Nucleation, Science, 327, 1243–1246, https://doi.org/10.1126/science.1180315, http://www.sciencemag.org/cgi/doi/10.1126/science.1180315, 2010.

Svensmark, H., Pedersen, J. O. P., Marsh, N. D., Enghoff, M. B., and Uggerhøj, U. I.: Experimental evidence for the role of ions in particle nucleation under atmospheric conditions, Proceedings of the Royal Society A, 463, 385–396, 2007.

Svensmark, H., Enghoff, M. B., and Pedersen, J. O. P.: Response of cloud condensation nuclei (> 50 nm) to changes in ion-nucleation, Physics Letters A, 377, 2343–2347, https://doi.org/10.1016/j.physleta.2013.07.004, 2013.

Tröstl, J. et al.: The role of low-volatility organic compounds in initial particle growth in the atmosphere, Nature, 533, https://doi.org/doi:10.1038/nature18271, 2016.

Vanhanen, J., Mikkilä, J., Lehtipalo, K., Sipilä, M., et al.: Particle Size Magnifier for Nano-CN Detection, Aerosol Science and Technology, 45, 533–542, https://doi.org/10.1080/02786826.2010.547889, http://www.tandfonline.com/doi/abs/10.1080/02786826.2010.547889, 2011.

von der Weiden, S.-L., Drewnick, F., and Borrmann, S.: Particle Loss Calculator – a new software tool for the assessment of the performance of aerosol inlet systems, Atmospheric Measurement Techniques, 2, 479–494, https://doi.org/10.5194/amt-2-479-2009, https://www.atmos-meas-tech.net/2/479/2009/, 2009.

Winkler, P. M., Steiner, G., Vrtala, A., Vehkamäki, H., et al.: Heterogeneous Nucleation Experiments Bridging the Scale from Molecular Ion Clusters to Nanoparticles, Science, 319, 1374–1377, https://doi.org/10.1126/science.1149034, http://science.sciencemag.org/content/319/5868/1374, 2008.

Yu, F. and Luo, G.: Simulation of particle size distribution with a global aerosol model: contribution of nucleation to aerosol and CCN number concentrations, Atmospheric Chemistry and Physics, 9, 7691–7710, https://doi.org/10.5194/acp-9-7691-2009, https://www.atmos-chem-phys.net/9/7691/2009/, 2009.

Yu, H., Dai, L., Zhao, Y., et al.: Laboratory observations of temperature and humidity dependencies of nucleation and growth rates of sub-3 nm particles, Journal of Geophysical Research: Atmospheres, 122, 1919–1929, https://doi.org/10.1002/2016JD025619, http://dx.doi.org/10.1002/2016JD025619, 2016JD025619, 2017.